MECHANISMS OF DEVELOPMENT XXX (2014) XXX–XXX

Available at www.sciencedirect.com

ScienceDirect

journal homepage: www.elsevier.com/locate/modo

Retinoic acid induced-1 (Rai1) regulates craniofacial and brain development in *Xenopus*

Raiha Tahir [a], *Allyson Kennedy* [b], *Sarah H. Elsea* [c], *Amanda J. Dickinson* [b,*]

[a] *Center of the Study of Biological Complexity, Virginia Commonwealth University, Richmond, VA 23284, USA*
[b] *Department of Biology, Virginia Commonwealth University, Richmond, VA 23284, USA*
[c] *Department of Molecular and Human Genetics, Baylor College of Medicine, One Baylor Plaza, MS NAB2015, Houston, TX 77030, USA*

ARTICLE INFO

Article history:
Received 4 March 2014
Received in revised form
16 May 2014
Accepted 19 May 2014
Available online xxxx

Keywords:
Rai1
Xenopus
Craniofacial
Brain

ABSTRACT

Retinoic acid induced-1 (RAI1) is an important yet understudied histone code reader that when mutated in humans results in Smith–Magenis syndrome (SMS), a neurobehavioral disorder accompanied by signature craniofacial abnormalities. Despite previous studies in mouse and human cell models, very little is known about the function of RAI1 during embryonic development. In the present study, we have turned to the model vertebrates *Xenopus laevis* and *Xenopus tropicalis* to better understand the developmental roles of Rai1. First we demonstrate that the Rai1 protein sequence is conserved in frogs, especially in known functional domains. By *in situ* hybridization we revealed expression of *rai1* in the developing craniofacial tissues and the nervous system. Knockdown of Rai1 using antisense morpholinos resulted in defects in the developing brain and face. In particular, Rai1 morphants display midface hypoplasia and malformed mouth shape analogous to defects in humans with SMS. These craniofacial defects were accompanied with aberrant neural crest migration and reduction in the size of facial cartilage elements. Rai1 morphants also had defects in axon patterns and decreased forebrain ventricle size. Such brain defects correlated with a decrease in the neurotrophic factor, *bdnf*, and increased forebrain apoptosis. Our results emphasize a critical role of Rai1 for normal neural and craniofacial development, and further the current understanding of potential mechanisms that cause SMS.

1. Introduction

Smith–Magenis syndrome (OMIM 182290, SMS) is a complex genetic disorder characterized by craniofacial abnormalities and neurobehavioral problems. SMS is attributed to a chromosome 17p11.2 deletion that includes *RAI1* (retinoic acid induced-1) or a mutation in *RAI1* (Bi et al., 2006; Elsea et al., 1997; Girirajan et al., 2006; Juyal et al., 1996; Slager et al., 2003). Craniofacial malformations are one of the most frequent and clinically recognizable features among SMS patients. Features include a broad square-shaped face, a flat nasal bridge, a tented upper lip, and midface hypoplasia (reviewed in Elsea and Girirajan (2008)). In addition, SMS patients have a host of neurobehavioral problems (Elsea and Girirajan, 2008), including sleep disturbance and autism spectrum disorder (ASD) (Laje et al., 2010). These clinical characteristics are consistent with observations in SMS mouse models, which show similar

* Corresponding author. Tel.: +1 857 334 5848.
E-mail address: ajdickinson@vcu.edu (A.J. Dickinson).
http://dx.doi.org/10.1016/j.mod.2014.05.004
0925-4773/

facial dysmorphisms and neurological problems (Bi et al., 2005a; Yan et al., 2007).

Experimental and computational studies provide evidence for RAI1 as a transcriptional regulator (Carmona-Mora et al., 2010; Carmona-Mora and Walz, 2010). Further, sequence analyses and experimental work revealed that the RAI1 protein contains a C-terminus PHD domain or finger that can interact with chromatin and potentially act as histone code reader (Carmona-Mora et al., 2010; Darvekar et al., 2013). However, little is known about the specific function of RAI1 during development. Studies in mouse have been hampered by the fact that null mutations of *rai1* are often lethal, and variation in genetic background is thought to cause significant variability in the phenotypes (Bi et al., 2007). Therefore, we have turned to *Xenopus* as a tool to uncover the developmental mechanisms regulated by Rai1. *Xenopus*, like zebrafish, has become recognized as a valuable tool for dissecting the developmental mechanisms underlying genes involved in human diseases (Fieber et al., 2012; Kaltenbrun et al., 2011; Khokha, 2012; Pratt and Khakhalin, 2013; Santoriello and Zon, 2012; Sive, 2011; Tropepe and Sive, 2003; Wilkins and Pack, 2013; Zon, 1999). Not only is *Xenopus* genetically very similar to humans (Hellsten et al., 2010; Showell and Conlon, 2007), it is also surprisingly similar anatomically to humans, especially during embryogenesis. Moreover, *Xenopus* has numerous advantages as a model system in which to identify and characterize cellular and developmental processes. For example, the *Xenopus* embryo develops externally unlike the mouse, and its early patterning and morphogenesis have been studied extensively (Khokha, 2012). Knockdown of specific gene products in the early embryo are titratable and routine. Therefore, the molecular and cellular pathways through which proteins function, in particular Rai1, can be easily elucidated using *Xenopus*.

In the present study, we establish *Xenopus* as a tool for understanding Rai1 function during development. We show conserved protein structure, expression patterns, and developmental requirements in frogs. Importantly, we also provide some insight into possible mechanisms by which decreased Rai1 results in craniofacial malformation and brain disorders. Specifically, Rai1 may modulate neural crest development, as well as neuronal survival.

2. Results

2.1. *RAI1 protein sequence and organization is conserved across vertebrates*

In all vertebrates examined, the Rai1 protein ranges from 202 to 214 kDa and contains conserved domains responsible for transcriptional activation (TAD), nuclear localization (NLS containing region), and chromatin remodeling (PHD finger or ePHD/ADD (extended plant homeodomain/ATRX-DMNT3-DNMT3L)domain) (Fig. 1A). A multiple alignment of human, mouse, both species of model frogs (*Xenopus tropicalis* and *Xenopus laevis*) and zebrafish indicates the organization of these domains is similar across vertebrates (Fig 1A). A more extensive analysis of by Darvekar et al. (Darvekar et al., 2013) reported similar findings; however, *Xenopus laevis* was not included in their analysis. Both *X. tropicalis* and *X. laevis* Rai1 share 44% and 42% over all identity, respectively, with the human RAI1 protein (Table 1). However, more local similarity was observed in the functional domains, especially in the PHD finger where there is a 65% and 68% shared identity with *X. tropicalis* and *X. laevis*, respectively (Table 1 and Suppl. Fig. 1A). We also compared the Rai1 sequence in the two species of frogs used in this study and determined that they are highly similar (~90% identity), with the exception of a 43 amino acid sequence which is missing at C-terminus of the *X .laevis* sequence (see Fig. 1A and Suppl. Fig. 1C). This could be due to the poor sequencing results in this region of the newly sequenced *X. laevis* genome. Therefore, a better comparison of the *X. laevis* Rai1 protein awaits better sequence and annotation of the *X. laevis* genome. Regardless, these results suggest that both *Xenopus* models have well conserved Rai1 protein sequences that reflect a shared function with each other and other vertebrates.

2.2. *Retinoic acid regulates rai1 expression during embryonic development*

rai1 was initially identified as gene induced by retinoic acid (Imai et al., 1995). Since retinoic acid is critical for many aspects of embryonic development, we first asked whether the expression level of *rai1* in *X. laevis* embryos changes in response to excess retinoic acid. We exposed embryos (at stage 23) to 2.5 μM of all-trans retinoic acid (ATRA) or dimethyl sulfoxide (DMSO) for 4 h at room temperature followed by quantitative RT-PCR to measure relative levels of *rai1* mRNA. Results indicate that *rai1* expression was increased by 3.91-fold in embryos treated with ATRA relative to the controls (Fig. 1B; $n = 20$ in 2 experiments). Similarly, we found that *rai1* was also induced by ATRA in *X. tropicalis* (data not shown). These are the first results to show that *rai1* is induced by retinoic acid in the developing embryo.

The short time window of ATRA exposure suggests the possibility that *rai1* is a direct target of retinoic acid signals. To provide further evidence of this possibility, we analysed the promoter region of *rai1* to determine whether retinoic acid receptor consensus sequences were present. Using Patch software, we determined that 54 candidate RAR binding sites (25 RAR-α, 19 RAR-β, 10 RAR-γ) were present in the 2 kb region upstream of the start site in *X. laevis rai1* (Fig. 1C). While experimental studies are necessary to validate these binding predictions, together with the expression data, this analysis strongly suggests that *rai1* is a direct target of retinoic acid in the developing frog embryo.

2.3. *rai1 mRNA is expressed in the developing brain and craniofacial structures during Xenopus development*

To gain insight into the developmental role of Rai1, we first examined the spatiotemporal expression of the mRNA by *in situ* hybridization. Since *rai1* is a large gene with regions of close homology to other transcriptional regulators (Darvekar et al., 2013), we used an RNA probe created from the 3′-UTR of the *X. tropicalis* gene (Carter et al., 2010). This probe does not have sequence similarity to any other genes,

Please cite this article in press as: Tahir, R. et al, Retinoic acid induced-1 (Rai1) regulates craniofacial and brain development in Xenopus, Mech. Dev. (2014), http://dx.doi.org/10.1016/j.mod.2014.05.004

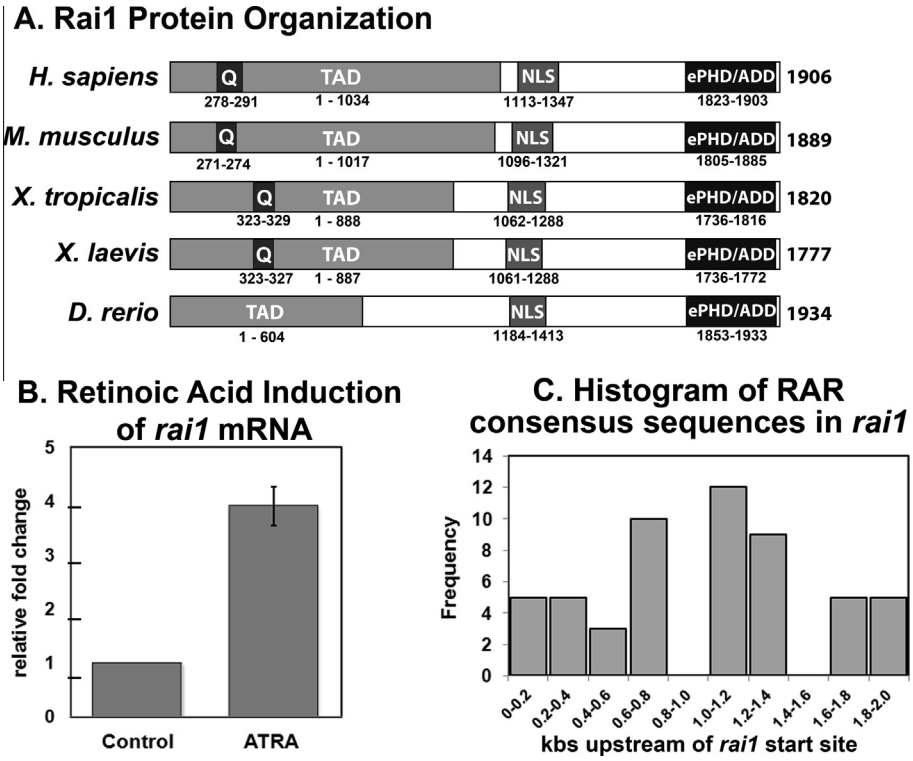

Fig. 1 – RAI1/Rai1 protein organization and induction by retinoic acid. (A) A schematic representation of the Rai1 protein in human, mouse, two frog species (*X. laevis* and *X. tropicalis*), and zebrafish. This illustrates that the organization of the primary protein domains, including the Trans-Activation Domain (TAD), Nuclear Localization Signal containing region (NLS; see Supplementary material Fig. S1B for details), and extended plant homeodomain (ePHD/ADD, also known as a PHD finger) are conserved in the species examined (see Supplementary material Fig. S1A for sequence alignment of the PHD finger). A 14 poly-glutamine stretch (Q) is found in humans and reduced glutamine stretches can also be found in a similar region of other species except zebrafish. The NLS region contains the first known nuclear localization sequence (Darvekar et al., 2013). Figure not to scale. (B) Retinoic acid induces expression of *rai1* during Xenopus development. Quantitative PCR of *rai1* mRNA after all-trans retinoic treatment (ATRA) at stage 23 showing significant 3.91-fold increase (t-test, $p = 0.0037$) relative to the control housekeeping gene (*ef1 alpha*). (C) Retinoic acid may directly regulate *rai1*. A histogram of RAR binding sites in a 2 kb region upstream of the *rai1* start site in *X. laevis* reveals the enrichment of retinoic acid receptor binding sites.

Table 1 – Comparison of human RAI1 full-length protein sequence and major domains with mice, frogs and zebrafish.

Species	Percent identity with *Homo sapiens*			
	Full-length	TAD	NLS	ePHD/ADD
Mus musculus	82	85	80	84
Xenopus tropicalis	44	49	42	65
Xenopus laevis	42	49	43	68
Danio rerio	27	35	23	58

Transcriptional activation domain (TAD), nuclear localization containing region (NLS); ePHD/ADD (extended plant homeodomain/ATRX-DMNT3-DNMT3L) domain.

and it demonstrated a specific expression pattern in *X. tropicalis* (Fig. 2A), as well as *X. laevis* (Supplementary material. Fig. S2A, B). Embryos labeled with a sense or control probe showed no staining (Supplementary material Fig. S2C, D). During neurulation (stage 18), *rai1* is expressed throughout the entire neural plate (Fig. 2Ai). While at stages 23–26, over the period of early morphogenesis, *rai1* is expressed in the developing muscle segments, CNS, eye, and in streams that resemble the migratory neural crest (Fig. 2Aii, iii arrows). By stage 33, *rai1* is also expressed in the branchial arches and the otic vesicle (Fig. 2Aiv). Additionally, a dorsal view of the embryo reveals distinct expression in the developing CNS at this stage (Fig. 2Av). Finally, as the jaw cartilage and mouth are forming (stage 41), *rai1* becomes ubiquitously expressed throughout the head (Fig. 2Avi). Transverse sections of these embryos reveals such labeling is confined to the mesenchyme

Please cite this article in press as: Tahir, R. et al, Retinoic acid induced-1 (Rai1) regulates craniofacial and brain development in Xenopus, Mech. Dev. (2014), http://dx.doi.org/10.1016/j.mod.2014.05.004

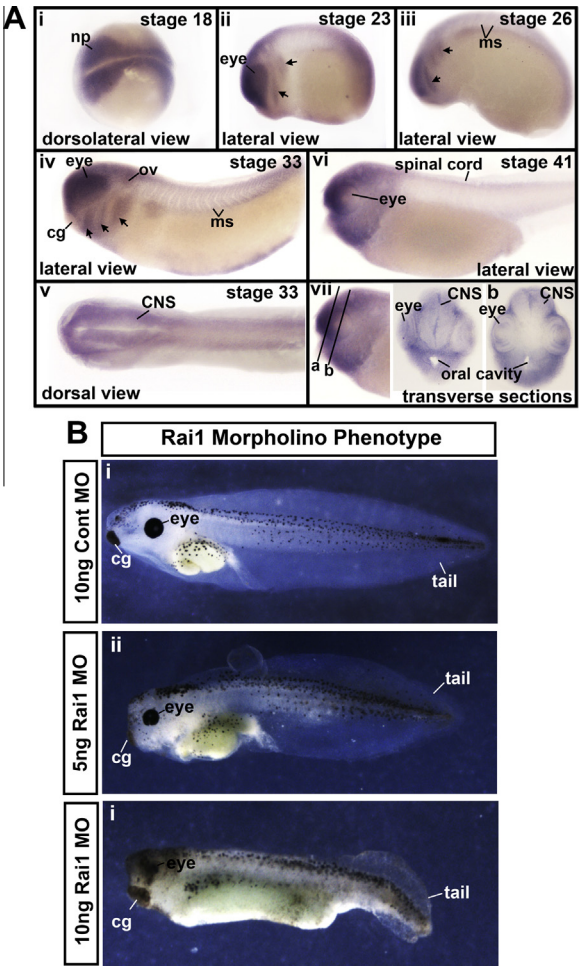

Fig. 2 – Expression and loss of function reveal a role for Rai1 in craniofacial and brain development. (A) *In situ* hybridization of *rai1* mRNA in *Xenopus tropicalis*. (i) Dorsolateral view at stage 18–19 revealing labeling throughout the developing nervous system. (ii) Lateral view of stage 23, revealing *rai1* in the presumptive migrating neural crest (arrows) and eye. (iii) Lateral view of stage 26 revealing *rai1* in the presumptive migrating neural crest (arrows). (iv) Lateral view of stage 33 revealing rai1 in the branchial arches (arrows) eye, optic vesicle (ov) and muscle segments (ms). (v) Dorsal view at stage 33 revealing *rai1* in the central nervous system (CNS). (vi) Lateral view at stage 41 revealing *rai1* throughout the head. (vii) Transverse sections through the head at stage 41 revealing that *rai1* is primarily located outside the CNS in the tissues of the face at this stage. Abbreviations, np; neural plate, ms; muscle segments, ov; otic vesicle, cg; cement gland, CNS; central nervous system. (B) Decreased function of Rai1 results in dramatic effects on *Xenopus laevis* development including craniofacial defects. (i) Lateral view of representative embryo at stage 42 injected with control morpholino (MO). (ii) Lateral view of representative embryo at stage 42 injected with 5 ng of MO. Defects include digestive tract, shortened tail and smaller head. (iii) Lateral view of representative embryo at stage 42 injected with 10 ng of Rai1 MO. There are severe defects in digestive tract, tail and head development.

and cranial neural crest derivatives in the head rather than the CNS and eyes (Fig. 2Avii, a,b). In summary, we demonstrate that *rai1* is expressed in the developing brain and craniofacial tissues consistent with a role in the formation of these structures.

2.4. *Decreased Rai1 protein results in abnormal embryonic development*

To determine how Rai1 regulates embryonic development, we used a targeted knockdown approach in *Xenopus*. In these experiments, we decreased the translation of Rai1 using antisense oligos stabilized with morpholino rings that bind to the mRNA (Morpholino (MO), Gene Tools). *X. laevis* embryos were injected at the one cell stage with various concentrations of a Rai1 MO or a standard control MO. We quantified the phenotypes in three experiments at each concentration. Control MO injections ranging from 1 to 20 ng had consistently less than 3% abnormal development. In most cases, we could not distinguish the difference between these and uninjected siblings (Fig. 2Bi). Injection of 5 ng of Rai1 MO produced a mild phenotype in 91% of the embryos. This mild phenotype included a slightly shorter body and an approximate 25% reduction in head and eye size viewed laterally ($n = 156$, 3 experiments, Fig. 2Biii). When 10 ng of Rai1 MO was injected, 89.8% of embryos were malformed. In these embryos a severely reduced head size (greater than 50% reduction), small eyes, abnormal pigment migration, malformed tail and under developed digestive tract were consistently observed ($n = 157$, 3 experiments, Fig. 2Bii). A small percentage (6.3%) of these embryos died before the analysis. 20 ng of Rai1 MO resulted in high percentages (>80%) embryonic death; and therefore, the phenotypes at these concentrations were not pursued (not shown). When 0.5–1 ng of this same morpholino was injected into *X. tropicalis* we saw similar phenotypes (data not shown) suggesting conservation of Rai1 function across the two species of frogs and specificity of the morpholino (Eisen and Smith, 2008).

To confirm the specificity Rai1 MO induced phenotype we injected another translation blocking morpholino (Rai1 MO2) targeting a different region of *rai1* mRNA. In three independent experiments ($n = 90$) we observed almost identical phenotypes at stages 40–42 (see Supplementary material Fig. S3A) suggesting that indeed decreased Rai1 results in specific developmental defects. In addition to confirm that our original Rai MO affected levels of Rai1 protein, we performed immunohistochemistry on stage 20 *X. laevis* Rai1 morphants using a human RAI1 antibody. Using pixel intensity of the immunofluorescence, we quantified the effect of the morpholino. While we saw significant staining throughout the control embryo, this was reduced by 2.16-fold ($p = 0.000116$, 2 experiments, $n = 10$) in the morphants, suggesting the morpholino was effective (Supplementary material Fig. S3B).

The general phenotypes observed upon Rai1 knockdown are consistent with a role for this protein in craniofacial and neural development; therefore, in the next sections, we focus on a deeper evaluation of the face and brain in Rai1 morphants.

Please cite this article in press as: Tahir, R. et al, Retinoic acid induced-1 (Rai1) regulates craniofacial and brain development in Xenopus, Mech. Dev. (2014), http://dx.doi.org/10.1016/j.mod.2014.05.004

2.5. *Decreased Rai1 alters facial size and shape during embryonic development*

Craniofacial abnormalities affecting the shape of the face and mouth are a hallmark of SMS in humans (reviewed in Elsea and Girirajan (2008)). In a qualitative analysis of craniofacial development in X. *laevis,* several abnormalities were noted. For example, Rai1 morphants have a narrower face, rounder mouth, and lack of upper jaw extension dorsal to the mouth (Fig. 3Ai–iv). It is also interesting to point out the apparent protrusion of the forehead where the forebrain forms as a result of midface hypoplasia (Fig. 3Aiv, outlined in white dots). Since craniofacial dimensions and shape were obviously affected in Rai1 knockdowns, we performed a quantitative analysis of the face in two additional experiments to better understand how Rai1 may function in craniofacial development and to make comparisons with humans with SMS and mouse mutants. In this analysis, traditional measurements and geometric morphometrics were combined to assess changes in size and shape of the face ($n = 20$ in 2 expts) (Kennedy and Dickinson, 2014).

One prominent characteristic of mice with decreased Rai1 function is a shorter snout length (Bi et al., 2005b; Yan et al., 2007). Therefore, we measured an analogous region of the embryonic frog face that incorporates the cartilages lining the base of the brain, nostrils, and upper jaw. The Rai1 morphant snout length was significantly decreased by 1.91-fold compared to the controls ($p = 1.25E-12$, Fig. 3Bi). SMS patients have midface hypoplasia and associated abnormalities in this region of the face. Therefore, we measured the area, width, and height of the midface region in X. *laevis* to determine if Rai1 has a conserved role in midface development. The midface area and width were reduced 1.38- and 1.44-fold, respectively, in the *rai1* morphants compared to controls ($p = 6.18E-10$ and $p = 1.17E-11$, respectively; Fig. 3Bii, iii). Conversely, in these morphants, the midface height was not

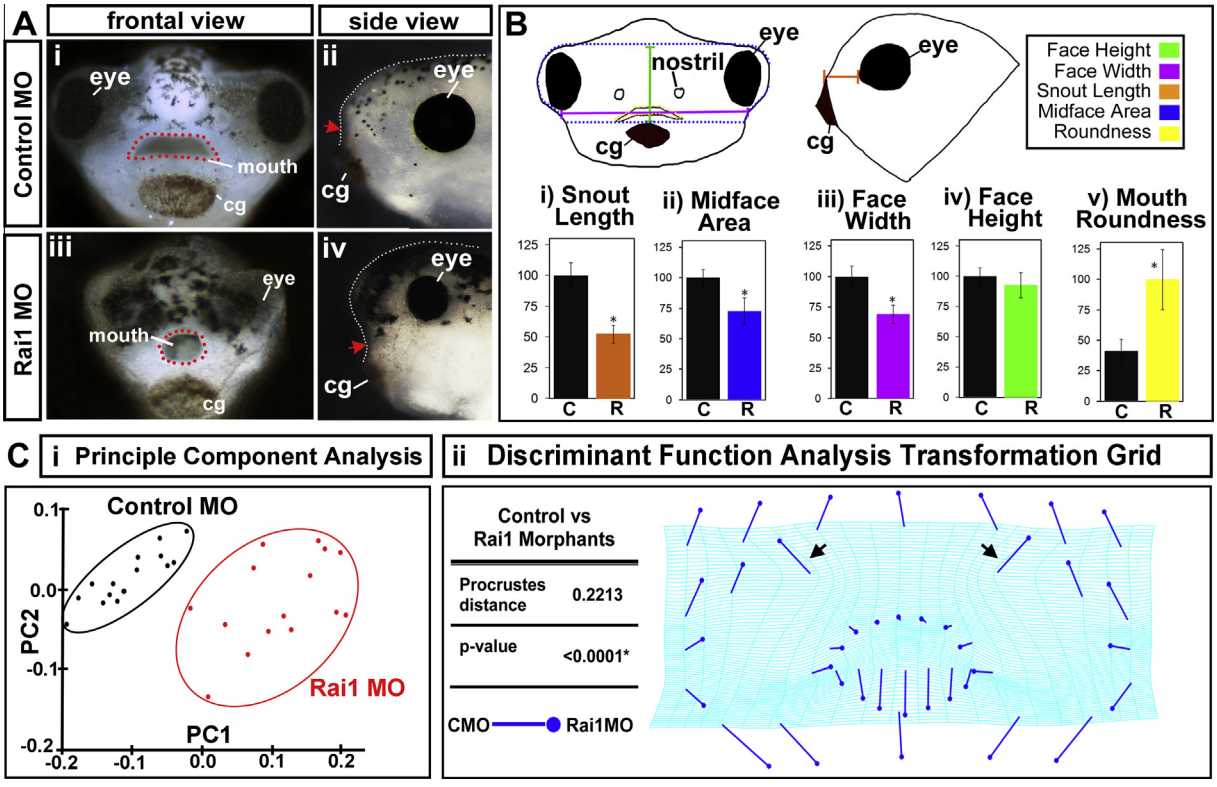

Fig. 3 – Rai1 is required for normal orofacial development. Rai1 morphants injected with 5 ng of morpholino were analyzed at stage 42. (A) Representative frontal views (i, iii) and lateral views (ii, iv) of embryos injected with 5 ng of Rai1 and control MO. The mouth is outlined in red dots (i and iii) or indicated with a red arrow (ii and iv). In lateral views (ii and iv) the head is outlined with white dots to emphasize the protruding forehead. The snout appears shorter and the mouth is smaller and rounder in the Rai1 morphants than controls. Abbreviations: cg; cement gland. (B) Traditional measurements of facial dimensions in Rai1 morphants verses controls. Schematics indicate where measurements were taken. Data as bar graphs (i–v), show statistically a shorter snout, smaller midface area, a narrower face, and rounder mouth. (C) Morphometric analysis of orofacial shape in Rai1 morphants supports tradition measurements and provides details of changes in orofacial shape. (i) Principal component analysis shows distinct separation of orofacial shapes in Rai1 morphants and controls. Control morphants are in black and Rai1 morphants are in red. (ii) Discriminant function analysis showing the statistically significant procrustes distance and *p*-value as well as the transformation grid of the changes in landmark location. Note the dramatic shift in nostril landmarks (arrows) and corresponding warping in the midface indicative of midface hypoplasia. Also notable is the shifts in mouth landmarks consistent with a rounder shape mouth.

Please cite this article in press as: Tahir, R. et al, Retinoic acid induced-1 (Rai1) regulates craniofacial and brain development in Xenopus, Mech. Dev. (2014), http://dx.doi.org/10.1016/j.mod.2014.05.004

significantly different ($p = 0.027$, Fig. 3Biv). SMS affected individuals also have a tented upper lip that changes the shape of the mouth opening. In *X. laevis*, the Rai1 morphants also have an abnormal mouth opening shape, where the mouth does not close and remains more rounded (see Fig. 3Aiii). Therefore, we quantified roundness using an inverse aspect ratio generated in Image J (Kennedy and Dickinson, 2014). Indeed, Rai1 morphants had a 2.44-fold rounder-shaped mouth opening compared to the controls ($p = 2.36E-09$, Fig. 3Bv). In summary, these data reveal that Rai1 morphants have narrowing in the midface region and a rounder mouth.

Since this traditional analysis does not provide a sophisticated view of how the shape of the embryonic orofacial region changes in response to reduced Rai1, we next used a morphometric analysis that we previously developed for frogs (Kennedy and Dickinson, 2014) to better define orofacial shape changes in Rai1 morphants. Thirty-eight landmarks were assigned coordinates as described previously (Kennedy and Dickinson, 2014) and then aligned via procrustes superimposition to eliminate information regarding size or orientation using MorphJ software (Klingenberg, 2011). The variance within each group was examined by performing a principal component analysis (PCA). By translating variables into orthogonal principal components, this multivariate statistical method describes the complexity of a sample while simultaneously reducing the number of variables (Abdi and Williams, 2010). The first two principal components account for the most variance within each group, and similar samples cluster together when these components are plotted against each other. Rai1 morphants were distinguished from controls along both the PC1 and PC2 axes (Fig. 3Ci). Individuals within the Rai1 morphant group were widely distributed, suggesting a large amount of variation. Such variance may be attributed to slightly different quantities or distribution of morpholino in each individual embryo, as well as other factors such as genetic background. Individuals in the control group were less widely distributed, but the variance can once again be explained by slight developmental differences in each embryo. To visualize the statistical differences in the shape of the orofacial region between Rai1 and control morphants, a discriminant function analysis (DFA) was performed. The procrustes distance was used to generate a statistical measure ($p < 0.001$) as well as a transformation grid to visualize the shape differences between the two groups (Fig. 3Cii). The lengths of the vectors illustrate how landmarks shift in the control (end of line) to the Rai1 morphants (closed circle). Dramatic shifts in the landmarks outlining the orofacial region indicate a narrowing of the face shape respective to the height (Fig. 3Cii). Also notable are the outward shift of the nasal landmarks (Fig. 3Cii, arrows) that reveal drastic abnormality in nostril position consistent with the failure of snout outgrowth. Shifts in the landmarks defining the dorsal edge of the mouth opening demonstrate the rounder shape of the mouth. In addition to vector shifts, the transformation grid also creates a warping pattern that illustrates shape change. Warping in the midface region is dramatic and consistent with midface hypoplasia in Rai1 morphants (Fig. 3Cii). The results of our DFA analysis revealed shape changes consistent with our qualitative observations and traditional size measurements such as narrow faces and increased mouth roundness. In summary, these results reveal size and shape changes in the frog Rai1 morphant embryo that are remarkably similar to craniofacial abnormalities in humans with SMS and mouse models, suggesting a conserved function for Rai1 in orofacial development.

2.6. Rai1 morphants have defects in neural crest migration and cartilage formation

While it is clear that abnormal facial shapes exist in humans, mice, and frogs deficient for Rai1, it remains unclear precisely why such malformation occurs. Since formation of the face depends largely on neural crest development, we first examined this important tissue in our Rai1 morphants using a well-established neural crest marker, *ap-2* (activating enhancer binding protein-2 alpha (de Croze et al., 2011; Winning et al., 1991)). In *X. laevis* Rai1 morphants, the pattern of *ap-2* expression was severely affected such that it appeared the neural crest was not migrating properly at stage 20 (Fig. 4A). When the pattern of *ap-2* was examined later (stage 30–32), we noticed that neural crest appeared to migrate but the pattern was abnormal in Rai1 morphants compared to controls (Fig. 4B). First we noted that while migration occurred, it seemed delayed. In addition, there could be fewer neural crest cells and the streams seemed to be less defined. To determine if the delayed migration effect was due to simply Rai1 morphants developing slower, Rai1 MO was injected into one cell at the 2-cell stage. In these embryos we also noticed that the pattern of ap-2 was abnormal on the injected side compared to the uninjected side similar to whole embryo injections (see Supplemental material Fig. S4).

To determine if the defective neural crest development we observed affected formation of its derivatives, we next examined the developing cartilage. Almost every identifiable cartilage element, especially the ethmoid plate, infrarostral, Meckel's, ceratohyal and gill cartilages was reduced in size in Rai1 morphants (Fig. 4C). Such reductions could account for the narrower face, midface hypoplasia, and misshapen mouth that we observed. In summary, we have shown that the neural crest does not develop correctly and cartilages are reduced in embryos with decreased Rai1. This is the first study to suggest that Rai1 is necessary for neural crest development and provides a mechanism to explain facial dysmorphism in SMS.

2.7. Decreased Rai1 function results in brain abnormalities and decreased expression of bdnf during embryonic development

In addition to facial abnormalities, humans with SMS also have a host of neurological problems that fall into the autism spectrum (Laje et al., 2010). Therefore, we examined brain structure and axon patterns in embryos with decreased Rai1. First, a neurofilament marker was used to reveal axons in Rai1 morphants at stage 42. Results clearly indicate a malformed pattern of axons throughout the craniofacial region in morphants compared to controls (Fig. 5A and B). Many of the nerve tracts into the face lacked a smooth trajectory (Fig. 5B). In addition, axons of Rai1 morphants had qualitatively more blebbing or beading than controls, suggesting the possibility

Please cite this article in press as: Tahir, R. et al, Retinoic acid induced-1 (Rai1) regulates craniofacial and brain development in Xenopus, Mech. Dev. (2014), http://dx.doi.org/10.1016/j.mod.2014.05.004

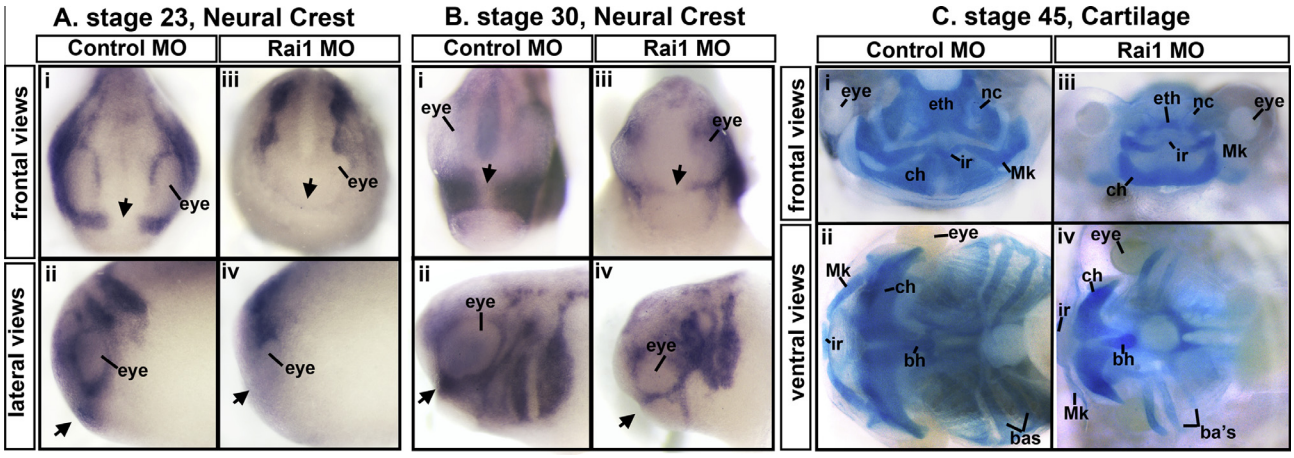

Fig. 4 – Rai1 is critical for neural crest migration and to establish correct cartilage size. Rai1 morphants injected with 5 ng of morpholino were used for analysis. (A) *in situ* hybridizations of the neural crest marker, *ap-2* in control (i, ii) and Rai1 morphants (iii, iv), showing an aberrant pattern of neural crest during early migration (stage 23). Arrows indicate position of the developing embryonic mouth for context. (B) *in situ* hybridizations of *ap-2* in control (i, ii) and Rai1 morphants (iii, iv), showing an aberrant pattern of neural crest after migration (stage 30). Arrows indicate position of the developing embryonic mouth for context. (C) Cartilage labeling by Alcian Blue in control (i, ii) and Rai1 morphants (iii, iv) illustrates a decreased size of cartilage elements at stage 45. Abbreviations: eth; ethmoid, nc; nasal capsule, MK; Meckel's, ir; infrarostral, ch; ceratohyal, ba; branchial, bh; basohyal.

of neural degeneration (Fig. 5B, arrow heads). Further, we also noticed that the structure of the brain appeared abnormal, especially the forebrain, in Rai1 morphants. One problem associated with modifications in brain structure is changes in the ventricle space (Gato and Desmond, 2009; Lowery and Sive, 2009). Therefore, we visualized the ventricle spaces in Rai1 morphants at stage 42 by injecting labeled dextran into the hindbrain ventricle using a technique commonly used for zebrafish (Gutzman and Sive, 2009). The results show that Rai1 morphants had a reduced, occluded, or absent forebrain ventricle (Fig. 5C and D). Attempting to fill the forebrain ventricle directly with high pressure was unsuccessful, suggesting that an occlusion was unlikely the cause of the defect.

To address whether the structural abnormalities in the forebrain and beading of the axon tracts in Rai1 morphants could be due to an increase in cell death, we quantified apoptosis at stage 33–34. An antibody that detected cleaved caspase-3 was utilized as an apoptotic marker (Duan et al., 2003). Results revealed that Rai1 morphants had a 3.6-fold increase in the number of apoptotic cells compared to the control morphants (p = 2.48E-10, Fig. 5E-G). On the other hand, there was no significant difference in the number of cleaved-caspase-3 positive cells in the face at this time point (p = 0.713, Fig. 5E–G).

One mechanism by which RAI1 could regulate neural development is via its modulation of brain derived neurotrophic factor (*bdnf*). Reduction of *Bdnf* has been reported in *Rai1* haploinsufficient mice (Burns et al., 2010), and Bdnf functions during development as neurotrophic factor supporting growth and survival of neurons (reviewed in Lindsay (1996)). Therefore, we hypothesized that decreased *bdnf* could account for at least some of the neural defects we observed in Rai1 morphants. To test this hypothesis, *bdnf* mRNA expression levels were measured in *X. laevis* Rai1 morphants at stage 25–26 (28 hpf) by quantitative RT-PCR. Our results indicated that *bdnf* mRNA was significantly decreased by 1.5-fold in Rai1 morphants compared to controls (Fig. 5H, 2 experiments).

In summary, we have shown that embryos deficient in Rai1 have a reduced forebrain ventricle space and abnormal patterns of nerve tracts. These defects may at least in part be due to a significant increase in apoptosis in the forebrain, which in turn could result from decreased levels of the neurotrophin Bdnf (Conover and Yancopoulos, 1997; Ichim et al., 2012). Future studies are aimed to solidify these connections.

3. Discussion

RAI1 is a relatively understudied but critical protein in development, since when mutated in humans it results in Smith–Magenis syndrome. Rai1 has a PHD finger domain that puts it in a class of important histone code readers such as trithorax, ING family, CHD4 and DNMT3 (Musselman and Kutateladze, 2009). The importance of this gene is further accentuated by the fact that most mouse embryos null for *rai1* die during embryonic development (Bi et al., 2005b). Also for this reason, the precise role of Rai1 during development has been difficult to study in mammals. Therefore, we utilized *Xenopus* as a tool to better understand how Rai1 functions during embryonic development.

3.1. *Rai1 expression and protein organization have conserved features across vertebrates*

Rai1 sequences across vertebrates harbor several protein modules characteristic of transcriptional regulators and chromatin readers. The transactivation domain (TAD) spanning the first half of the protein sequence has a predicted role of

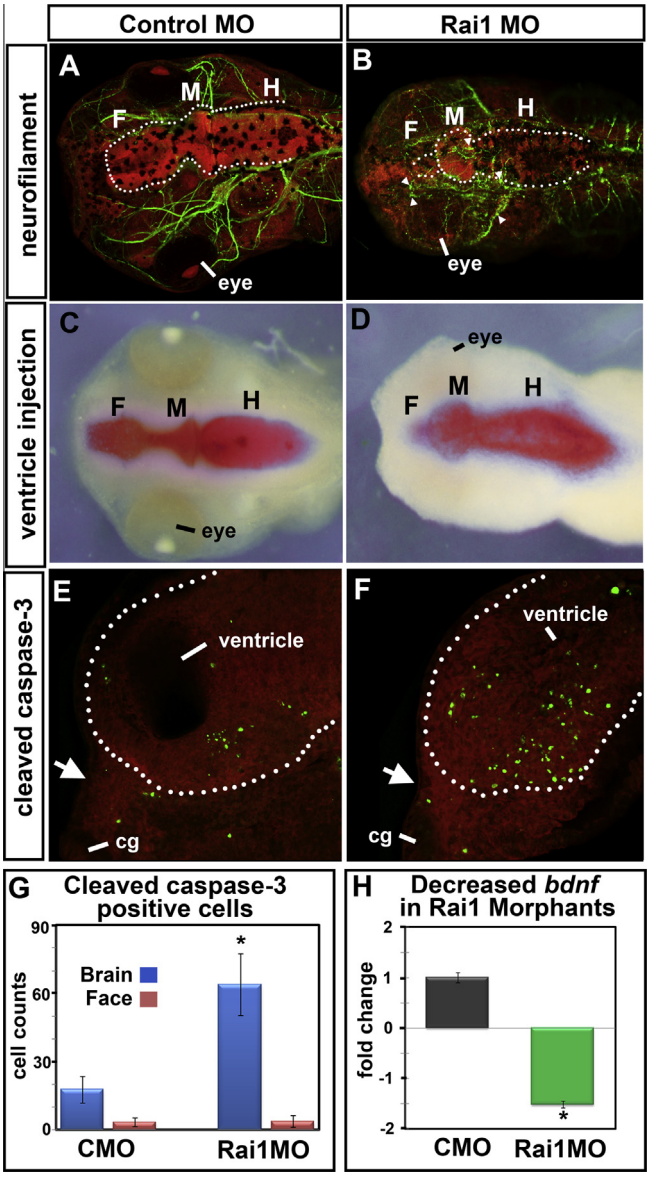

Fig. 5 – Decreased Rai1 results in defects in axon patterns, brain morphology, increased forebrain apoptosis and decreased *bdnf* expression. Rai1 morphants injected with 5 ng of morpholino were used for each analysis. (A, B) Dorsal view of representative tadpoles (stage 42) labeled with a neurofilament marker (3A10) showing aberrant axon patterns and axonal beading in Rai1 morphants (arrowheads). The brain is outlined with white dots to provide context. (C, D) Dorsal view of representative tadpoles (stage 42) where the ventricles were injected with Texas Red labeled dextran. Fluorescent images were superimposed onto the light micrographs to provide context. Results show that Rai1 morphants have dramatically decreased ventricle space in the forebrain. (E, F) A marker of apoptosis, cleaved caspase-3 (green) reveals increased cell death in the forebrain of Rai1 morphants. Shows a compressed z-stack of a midline sagital section at stage 33–34. Counterstained with nuclear marker (propidium iodide; red). The brain is outlined with white dots and the position of the developing embryonic mouth is indicated by a white arrow for context. (G) Bar graph of the average number of cleaved caspase-3 positive cells showing a significant difference (t tests, brain; $p = 2.48E\text{-}10$, face; $p = 0.713$) in the brain (star) but not in the face. (H) qPCR analysis of *bdnf* expression in Rai1 morphants at stage 25–26 (28 hpf). Expression was normalized to *ef1alpha* and presented as a fold change compared to control. Results indicate a statistically significant negative 1.5-fold change (t test, $p = 0.0049$) in Rai1 morphants.

conferring target gene specificity (Bi et al., 2005a; Hu et al., 2007). Downstream from the TAD region lies an NLS containing region, having predicted sequences important for nuclear localization of Rai1 (Supplementary material Fig. S1B) (Carmona-Mora et al., 2010). The ePHD/ADD domain is a PHD finger characterized as a histone code reader (Musselman and Kutateladze, 2009). While, the overall identity of human RAI1 is 42% and 44% when compared to

Please cite this article in press as: Tahir, R. et al, Retinoic acid induced-1 (Rai1) regulates craniofacial and brain development in Xenopus, Mech. Dev. (2014), http://dx.doi.org/10.1016/j.mod.2014.05.004

X. laevis and *X. tropicalis*, respectively, our analysis indicates that these functional domains share higher sequence identity. This is especially true for the PHD finger which recent binding studies have confirmed its ability to bind to nucleosomes (Darvekar et al., 2013). This study emphasizes a potential importance for RAI1 in mediating interactions between chromatin, chromatin modulators and transcriptional regulators (Darvekar et al., 2013).

We also determined that *rai1* has at least a partially conserved expression pattern during development. In both *Xenopus* and mice, the branchial (or pharyngeal) arches and otic vesicles are *rai1* positive. However, we also observed *rai1* mRNA in the brain, neural crest and eye in *Xenopus*. While *rai1* is expressed in the adult and newborn mouse brain the expression of this gene has not been closely examined in embryonic brain, neural crest or eye in mammals (Bi et al., 2005b; Cao et al., 2013).

Based on sequence analysis of the Rai1 protein and overlap in *rai1* mRNA expression it is likely that Rai1 has shared developmental functions in *Xenopus*.

3.2. A role for RAI1 in vertebrate craniofacial development may involve neural crest

Humans with SMS have a set of craniofacial abnormalities that include midface hypoplasia, depressed nasal bone, everted or tented upper lip, and upslanting palpebral fissures (Elsea and Girirajan, 2008). Many of these abnormalities can be attributed to a reduction in the development of the maxillary and frontonasal prominences that form most of the structures of the midface. It would seem counterintuitive then that these features would be accompanied by a wide or broad face and hypertelorism. However, it has been proposed that in such cases the nasal capsule does not form which then leads to a failure in normal medial orbital migration and an apparent widening of the face (Renato Ocampo and Persing, 1997). Similar midface abnormalities have also been reported in mice, where there is a shorter and broader snout that is consistent with a reduction in the nasal bone. In our study, we demonstrate analogous craniofacial abnormalities in Rai1 *Xenopus* morphants. For example, decreased Rai1 resulted in midface hypoplasia and malformed mouth shape. Other craniofacial abnormalities reported in SMS include frontal bossing and micrognatia, and analogous defects were also observed in *Xenopus*. Consistent with the orofacial size and shape changes are reductions in the orofacial cartilages in *Xenopus*. Thus, reduction of Rai1 results in analogous craniofacial defects in humans, mice and *Xenopus* further supporting a conserved role for Rai1 during development.

In this study, we are the first to identify a potential mechanism by which RAI1 deficiency affects craniofacial development. Such a mechanism includes a role for Rai1 in neural crest development. Not only did we identify *rai1* mRNA in what appeared to be migratory neural crest, but we also revealed abnormalities in the cranial neural crest in Rai1 morphants. Further studies are required to determine how precisely Rai1 functions in the development of this important tissue.

Craniofacial abnormalities can often be attributed to problems with neural crest development. For example, neural crest defects have also been reported in other syndromes that share common features with SMS such as Williams, DiGeorge, fragile X, Prader–Willi, and Down syndromes (Barnett et al., 2012; Hittner et al., 1982; Kochilas et al., 2002; Lim et al., 2005; Roper et al., 2009; Wurdak et al., 2005). Thus, our study lends support to the hypothesis that craniofacial deformities associated with many human congenital diseases are a result of abnormalities in neural crest development, migration or differentiation.

3.3. RAI1 is important for brain development in Xenopus

Neurological problems are also a common feature of SMS and include mild-to-moderate intellectual disability, self-injurious and maladaptive behaviors, as well as sleep disorders. Individuals with SMS also display characteristics similar to autism (Laje et al., 2010). Similarly, mice with lower levels of Rai1 (*Rai1*$^{+/-}$) had an abnormal electroencephalogram, and overt seizures were observed in a subset of these mice (Bi et al., 2007). The few *Rai1 null* mice that survive displayed more severe neurobehavioral abnormalities including hind limb clasping, overt seizures, motor impairment and context- and tone-dependant learning deficits. Mice with deficiencies in Rai1 also display abnormal social behaviors (Girirajan and Elsea, 2009). In *Xenopus* Rai1 morphants, we uncovered severe abnormalities in brain structure and axon paths, especially in the developing forebrain region. Such abnormalities could be due to the 3-fold increase in apoptosis in the brain. Certainly, cell death can account for the axonal beading we observed, which is a common characteristic of neurons after injury or in neurodegenerative diseases (Wang et al., 2012; Takeuchi et al., 2005). Increased apoptosis can also dramatically change the overall brain structure. Other similar disorders, such as Down syndrome, are associated with increased apoptosis in the brain (Seidl et al., 2001) and changes in embryonic brain structure (Jernigan and Bellugi, 1990; Yamada et al., 2006).

The increased apoptosis in *Xenopus* brain development also correlates with a reduction in an important neurotrophic factor *bdnf*. In mice, *bdnf* in the hypothalamus is a downstream target of Rai1 and its reduction is associated with obesity and altered fat distribution in the adult. Bdnf is well-known for its role in neuron survival and differentiation (Casaccia-Bonnefil et al., 1999; Ichim et al., 2012). In fact, others have shown that decreased Bdnf in *Xenopus* correlates with a 3-fold increase in apoptosis, similar to what we find in our Rai1 morphants (Huang et al., 2007). Thus, one mechanism by which Rai1 may be acting is modulating *bdnf* levels that insure neuronal survival during development. It would be interesting to determine if exogenous Bdnf can ameliorate the Rai1 morphant neural problems.

3.4. Rai1 is induced by retinoic acid during embryonic development

rai1 was first cloned as a novel gene upregulated in p19 cells in the presence of retinoic acid (Imai et al., 1995). We are the first to demonstrate that excess retinoic acid also enriches *rai1* in the developing embryo. Retinoic acid is indispensible for the development of numerous tissues and

Please cite this article in press as: Tahir, R. et al, Retinoic acid induced-1 (Rai1) regulates craniofacial and brain development in Xenopus, Mech. Dev. (2014), http://dx.doi.org/10.1016/j.mod.2014.05.004

organs, including the nervous system and craniofacial region (reviewed in Glover et al. (2006); Mark et al. (2004)). Therefore, it is not surprising then that Rai1 may be involved in the development the brain and face. In *Xenopus*, we find there is considerable overlap in roles of Rai1 and retinoic acid. For example, retinoic acid is necessary for the correct timing of neural crest emigration (Martinez-Morales et al., 2011), neural patterning (Chen et al., 2001), and branchial arch specification (Mark et al., 2004). Knockdown of the RA-synthesizing enzyme Raldh2 shares some similarities in orofacial phenotypes with Rai1 morphants (Kennedy and Dickinson, 2012). For example, Raldh2 morphants also have midface hypoplasia and narrowing of the face. However, Raldh2 and Rai1 morphants are not identical, likely due to the fact that *rai1* expression does not completely overlap Raldh2 during embryogenesis. Further, retinoic acid also regulates the expression of many other genes in the orofacial region ((Arima et al., 2005; Kennedy and Dickinson, 2012), Dickinson lab unpublished data).

In future studies, we might ask how Rai1 functions in the retinoic acid signaling network. Our promoter analysis suggests the possibility that retinoic acid directly regulates *rai1* expression, which in turn could initiate a cascade of transcriptional regulation. RAI1 may accomplish such regulation epigenetically since it can bind nucleosomes and histones (Darvekar et al., 2013). Xenopus could be an ideal system in which to dissect the mechanism by which Rai1 regulates downstream targets in the developing embryo.

3.5. Conclusion

In summary, our results suggest a conserved role for Rai1 during vertebrate craniofacial and neural development. Importantly, this work in Xenopus has provided some insight into the possible mechanisms by which depleted levels of RAI1 result in neurological and craniofacial problems in persons with SMS. Future studies will be aimed at understanding how Rai1 interacts with transcriptional networks important for both neural crest and neural development. Further, since Rai1 has been identified as a candidate histone reader it is of great interest to identify how this protein works together with chromatin modulators and the transcriptional machinery to regulate such networks. We have also shown that retinoic acid indeed induces *rai1* expression during development, however the sequence of events leading to this induction still remains to be elucidated. Here, we have shown that Xenopus is a valuable tool for dissecting the molecular mechanisms of Rai1 function during development. Future work in frogs regarding *rai1* induction and epigenetic roles may also prove valuable for uncovering therapeutics for the RAI1 haploinsufficiency observed in SMS.

4. Materials and methods

4.1. Computational analysis of the RAI1 protein and promoter

Full-length rai1 protein sequences for selected organisms were retrieved from NCBI as follows: *H. sapien* RAI1 (NP_109590.3), *M. musculus* Rai1 (AAT28187.1), *X. tropicalis* Rai1 (XP_002935900.1), and *D. rerio* rai1 (XP_005171718.1). *X. laevis* Rai1 protein sequence was obtained by performing a BLAST search of the *X. laevis* Genome Assembly version 7.1 (http://gbrowse.xenbase.org/fgb2/gbrowse/xl7_1/) and Assembly XenVis 2.0 (http://*Xenopus*.lab.nig.ac.jp/) with the *X. tropicalis rai1* coding sequence (XM_002935854.2). The resulting incomplete sequences from the two assemblies were overlapped to obtain a contiguous coding sequence, which was translated using the ExPASy Translate tool (http://web.expasy.org/translate/). To determine the coordinate location of rai1 TAD, Poly-glutamine, NLS, and PHD domains for each organism, we used the previously characterized human RAI1 protein structure as a reference (Carmona-Mora et al., 2010). The BLASTp program was used to align the amino acid sequence for each human RAI1 domain with the full-length rai protein from each organism to locate a similar region. Percent identity between corresponding domains was also obtained during this analysis.

The 2 kb sequence upstream of the *X. laevis rai1* start site was exported from the XenVis 2.0 genome browser. The sequence was scanned for transcription factor binding sites (vertebrate sites; minimum site length = 4) using the PATCH v1.0 tool (Chen et al., 2005). From the output, the frequency of RAR binding sites was determined for every 200 bp stretch using Excel.

4.2. Embryos

Xenopus laevis embryos were obtained and cultured using standard methods (Sive et al., 2000). Embryos were staged according to Nieuwkoop and Faber (Nieuwkoop and Faber, 1967).

4.3. In situ hybridization

In situ hybridizations were performed as described Sive et al. (2000), omitting the proteinase K treatment. In vitro reverse transcription from plasmids containing *rai1* (CX939626.1, from Openbiosystems, EXT1168-98020163) and *ap-2* (Winning et al., 1991) was utilized to create RNA *in situ* hybridization probes (antisense and sense probes). After whole mount labeling of stage 41, it was unclear where the probes were localized and therefore we sectioned these embryos with a vibratome at 75 μm.

4.4. Morpholinos and all-trans retinoic acid treatment

Antisense morpholinos (MOs)(Summerton, 2007) were purchased from Genetools. The Rai1 morpholino sequence used for the all experiments in this study is '5-ACCTTTCCCGAAAAGACTGCATGGC-3′. This was injected into numerous batches of embryos to pinpoint appropriate concentrations and determine if there was a reproducible phenotype. Once this was achieved three experiments were then performed and percentages of phenotypes calculated. A second translation blocking morpholino (Rai1 MO2) targeting a different sequence '5-GGGATTTTTCTGCTCCTATAAGCCA-3′ was used to confirm specificity in three independent experiments.

Please cite this article in press as: Tahir, R. et al, Retinoic acid induced-1 (Rai1) regulates craniofacial and brain development in Xenopus, Mech. Dev. (2014), http://dx.doi.org/10.1016/j.mod.2014.05.004

The "standard control morpholino" is as published by Genetools. Embryos at 1–2 cell stage were injected with 1–10 nL of MOs using an Ependorf micro-pressure injector and a glass pulled capillary tubes, as described Tandon et al. (2012).

Embryos (stage 23) were bathed in 2.5 μM all-trans retinoic acid (ATRA, Sigma (R2625)) combined with 1% DMSO in 0.1X MBS (Modified Barth's Saline, ph7.8) in culture dishes ($n = 20$ embryos in 2 experiments). Controls consisted of 1% DMSO alone. After a 4-h treatment, embryos were washed (3 times, 10 min each in 0.1X MBS) and transferred into 1 ml of Trizol reagent for quantitative RT-PCR.

4.5. *Quantitative RT-PCR*

RNA was extracted from *Xenopus laevis* embryos in Trizol (Invitrogen) as described previously (Dickinson and Sive, 2009; Kennedy and Dickinson, 2012). Briefly, standard Trizol extraction was followed by a lithium chloride solution (Ambion) precipitation and cDNA was prepared using the Omniscript Kit (Qiagen). Quantitative PCR was performed using a Mastermix containing Sybr Green (Sensifast, Bioline) and the Biorad CFX96 thermocycler. Primer validation using the standard curve method was performed and RT(−) was included for every primer and condition to set thresholds. The delta–delta–CT method was used to calculate relative quantities of product and (elongation factor-1 alpha (*ef1-alph* housekeeping gene served to normalize data. Normalized data was evaluated for significant differences using a student *t*-test. Primer sequences for *ef1 alpha*, *rai1* and *bdnf* are available upon request.

4.6. *Immunohistochemistry and Alcian blue staining*

Immunohistochemistry (IHC) was performed on either whole embryos or vibratome sections (75 μm) as described Dickinson and Sive (2006); Kennedy and Dickinson (2012). Embryos fixed in freshly made 4% PFA for 2–4 h at room temperature, washed in PBT and then sectioned by embedding in 4.5% low-melt agarose (SeaPlaque GTG, Cambrex) and cut with a 5000 Series Vibratome at 75–100 μm. Primary antibodies included a rabbit polyclonal anti-cleaved caspase-3 (Cell Signaling, 9661S, diluted 1:1000), rabbit polyclonal human RAI1 (generated by Alpha Diagnostic International for the Elsea lab, diluted 1:100 for further details see Supplementary material) and *Xenopus* monoclonal antibody that detects a Xenopus neurofilament (Developmental Studies Hybridoma Bank, 3A10, diluted 1:100). Appropriate secondary AlexaFluor 488 antibodies (Invitrogen) were diluted 1:500. Counterstain included 0.1% propidium iodide (Sigma, P4864). Confocal images of 50 μm depths were collected using the Nikon C1 confocal. Z-stacks were volume rendered using the accompanied Nikon C1-EZ software.

Cartilage was stained using standard protocols (Taylor, 1985) with some modifications, as we described previously (Kennedy and Dickinson, 2012). Briefly, tadpoles were fixed in Bouins fixative overnight at 4 °C and then washed in 70% ethanol. They were immersed in Alcian Blue stain for 3–4 days at RT. Embryos were washed in 1% HCl in 70% ethanol for 1–2 days and cleared in 2% potassium hydroxide in glycerol.

4.7. *Ventricle injections*

Ventricle injections were modified from procedures published for zebrafish (Gutzman and Sive, 2009). Embryos were fixed overnight in 4% PFA and then bleached in 10% H_20_2 (in PBS) until the pigment was eliminated. Embryos were then immobilized in modeling clay and PBS. Texas Red labeled dextran (Molecular Probes, D-1863) was "microinjected" into the hindbrain ventricle space using constant flow at low pressure settings. Higher pressure injections and injections directly into the forebrain were used to test for occlusions. Fluorescent images were overlaid on the bright field images in Photoshop (Adobe, Inc) to provide context.

4.8. *Analysis of craniofacial dimensions and geometric morphometrics*

Quantification of the Xenopus face was performed as described (Kennedy and Dickinson, 2014). Axiovision40V.4.8.1.0 software (Zeiss) was used to perform all standard measurements. On lateral images of tadpole faces, the snout length, which is from the bottom of the eye to the most anterior point on the face, above the cement gland, was measured. On frontal images of tadpole faces, the midface area was measured as the region between the top of the eyes to the top of the cement gland and the left and right lateral peripheries of the face. Facial width was measured from each lateral periphery of the face, just below the eyes. Facial height was measured as the distance between the top of the eyes and the top of the cement gland at the midline. ImageJ software (NIH) was used to measure the roundness of the mouth by outlining the mouth and applying the following inverse aspect ratio: *4*area/(π*major_axis^2)*. Data collected for the treatment groups were scaled so that the greatest average equaled 100. This allowed us to graphically compare all the measurements. Student *t*-tests in Excel (Microsoft) were used to determine statistical significance between *rai1* and control morphants.

To perform a morphometric analysis of the orofacial region, discrete landmarks of the orofacial region were established on tadpole faces as described (Anatomical Record). A total of 38 orofacial landmarks were placed on tadpole faces using the Pointpicker plugin of ImageJ (NIH). Facial landmarks 1–20 outlined the midface region from the center of the eyes to the top of the cement gland. Landmarks 21 and 22 were the center of each nostril, and landmarks 23–38 outlined the mouth opening. The coordinates of all of these landmarks were analyzed in MorphoJ 1.05f (Klingenberg et al., 2010). A procrustes superimposition was implemented to remove information concerning scale or size, position, and orientation. Variance within each group was determined by performing a principal component analysis (PCA), and a bivariate plot generated. Then we performed a canonical variate analysis (CVA) to visualize the statistical shape differences. This analysis was visualized as a plot of the first and second canonical variates as well as transformation grids. In these grids, the closed circle of the vectors was set as the treatment group and the line of the vector, then, represented the relative change in landmark position compared to the control

Please cite this article in press as: Tahir, R. et al, Retinoic acid induced-1 (Rai1) regulates craniofacial and brain development in Xenopus, Mech. Dev. (2014), http://dx.doi.org/10.1016/j.mod.2014.05.004

treatment group. The scale factor for the CVA transformation grids was set to the default.

Funding

This work was supported by start-up monies from Virginia Commonwealth University (A. Dickinson and S.H. Elsea), a grant from the Virginia Academy of Sciences (R. Tahir), and a grant from the Smith–Magenis Research Foundation (S.H. Elsea).

Appendix A. Supplementary data

Supplementary data associated with this article can be found, in the online version, at http://dx.doi.org/10.1016/j.mod.2014.05.004.

REFERENCES

Abdi, H., Williams, L.J., 2010. Principal component analysis. WIREs. Computational Statistics 2.

Arima, K., Shiotsugu, J., Niu, R., Khandpur, R., Martinez, M., Shin, Y., Koide, T., Cho, K.W., Kitayama, A., Ueno, N., Chandraratna, R.A., Blumberg, B., 2005. Global analysis of RAR-responsive genes in the *Xenopus neurula* using cDNA microarrays. Dev. Dyn. 232, 414–431.

Barnett, C., Yazgan, O., Kuo, H.C., Malakar, S., Thomas, T., Fitzgerald, A., Harbour, W., Henry, J.J., Krebs, J.E., 2012. Williams syndrome transcription factor is critical for neural crest cell function in *Xenopus laevis*. Mech. Dev. 129, 324–338.

Bi, W.M., Ohyama, T., Nakamura, H., Yan, J., Visvanathan, J., Justice, M.J., Lupski, J.R., 2005. Inactivation of Rai1 in mice recapitulates phenotypes observed in chromosome engineered mouse models for Smith–Magenis syndrome. Hum. Mol. Genet. 14, 983–995.

Bi, W., Ohyama, T., Nakamura, H., Yan, J., Visvanathan, J., Justice, M.J., Lupski, J.R., 2005a. Inactivation of Rai1 in mice recapitulates phenotypes observed in chromosome engineered mouse models for Smith–Magenis syndrome. Hum. Mol. Genet. 14, 983–995.

Bi, W., Saifi, G.M., Girirajan, S., Shi, X., Szomju, B., Firth, H., Magenis, R.E., Potocki, L., Elsea, S.H., Lupski, J.R., 2006. RAI1 point mutations, CAG repeat variation, and SNP analysis in non-deletion Smith–Magenis syndrome. Am. J. Med. Genet. A 140, 2454–2463.

Bi, W., Yan, J., Shi, X., Yuva-Paylor, L.A., Antalffy, B.A., Goldman, A., Yoo, J.W., Noebels, J.L., Armstrong, D.L., Paylor, R., Lupski, J.R., 2007. Rai1 deficiency in mice causes learning impairment and motor dysfunction, whereas Rai1 heterozygous mice display minimal behavioral phenotypes. Hum. Mol. Genet. 16, 1802–1813.

Burns, B., Schmidt, K., Williams, S.R., Kim, S., Girirajan, S., Elsea, S.H., 2010. Rai1 haploinsufficiency causes reduced Bdnf expression resulting in hyperphagia, obesity and altered fat distribution in mice and humans with no evidence of metabolic syndrome. Hum. Mol. Genet. 19, 4026–4042.

Cao, L., Molina, J., Abad, C., Carmona-Mora, P., Cardenas Oyarzo, A., Young, J.I., Walz, K., 2013. Correct developmental expression level of Rai1 in forebrain neurons is required for control of body weight, activity levels and learning and memory. Hum. Mol. Genet..

Carmona-Mora, P., Walz, K., 2010. Retinoic acid induced 1, RAI1: a dosage sensitive gene related to neurobehavioral alterations including autistic behavior. Curr. Genomics 11, 607–617.

Carmona-Mora, P., Encina, C.A., Canales, C.P., Cao, L., Molina, J., Kairath, P., Young, J.I., Walz, K., 2010. Functional and cellular characterization of human Retinoic Acid Induced 1 (RAI1) mutations associated with Smith–Magenis syndrome. BMC Mol. Biol. 11.

Carter, B.S., Fletcher, J.S., Thompson, R.C., 2010. Analysis of messenger RNA expression by in situ hybridization using RNA probes synthesized via in vitro transcription. Methods 52, 322–331.

Casaccia-Bonnefil, P., Gu, C., Chao, M.V., 1999. Neurotrophins in cell survival/death decisions. Adv. Exp. Med. Biol. 468, 275–282.

Chen, Y., Pollet, N., Niehrs, C., Pieler, T., 2001. Increased XRALDH2 activity has a posteriorizing effect on the central nervous system of *Xenopus embryos*. Mech. Dev. 101, 91–103.

Chen, J., Call, G.B., Beyer, E., Bui, C., Cespedes, A., Chan, A., Chan, J., Chan, S., Chhabra, A., Dang, P., Deravanesian, A., Hermogeno, B., Jen, J., Kim, E., Lee, E., Lewis, G., Marshall, J., Regalia, K., Shadpour, F., Shemmassian, A., Spivey, K., Wells, M., Wu, J., Yamauchi, Y., Yavari, A., Abrams, A., Abramson, A., Amado, L., Anderson, J., Bashour, K., Bibikova, E., Bookatz, A., Brewer, S., Buu, N., Calvillo, S., Cao, J., Chang, A., Chang, D., Chang, Y., Chen, Y., Choi, J., Chou, J., Datta, S., Davarifar, A., Desai, P., Fabrikant, J., Farnad, S., Fu, K., Garcia, E., Garrone, N., Gasparyan, S., Gayda, P., Goffstein, C., Gonzalez, C., Guirguis, M., Hassid, R., Hong, A., Hong, J., Hovestreydt, L., Hu, C., Jamshidian, F., Kahen, K., Kao, L., Kelley, M., Kho, T., Kim, S., Kim, Y., Kirkpatrick, B., Kohan, E., Kwak, R., Langenbacher, A., Laxamana, S., Lee, C., Lee, J., Lee, S.Y., Lee, T.H., Lee, T., Lezcano, S., Lin, H., Lin, P., Luu, J., Luu, T., Marrs, W., Marsh, E., Min, S., Minasian, T., Misra, A., Morimoto, M., Moshfegh, Y., Murray, J., Nguyen, C., Nguyen, K., Nodado 2nd, E., O'Donahue, A., Onugha, N., Orjiakor, N., Padhiar, B., Pavel-Dinu, M., Pavlenko, A., Paz, E., et al, 2005. Discovery-based science education: functional genomic dissection in *Drosophila* by undergraduate researchers. PLoS Biol. 3, e59.

Conover, J.C., Yancopoulos, G.D., 1997. Neurotrophin regulation of the developing nervous system: analyses of knockout mice. Rev. Neurosci. 8, 13–27.

Darvekar, S., Rekdal, C., Johansen, T., Sjottem, E., 2013. A phylogenetic study of SPBP and RAI1: evolutionary conservation of chromatin binding modules. PLoS One 8, e78907.

de Croze, N., Maczkowiak, F., Monsoro-Burq, A.H., 2011. Reiterative AP2a activity controls sequential steps in the neural crest gene regulatory network. Proc. Natl. Acad. Sci. U.S.A. 108, 155–160.

Dickinson, A.J., Sive, H., 2006. Development of the primary mouth in *Xenopus laevis*. Dev. Biol. 295, 700–713.

Dickinson, A.J., Sive, H.L., 2009. The Wnt antagonists Frzb-1 and crescent locally regulate basement membrane dissolution in the developing primary mouth. Development 136, 1071–1081.

Duan, W.R., Garner, D.S., Williams, S.D., Funckes-Shippy, C.L., Spath, I.S., Blomme, E.A., 2003. Comparison of immunohistochemistry for activated caspase-3 and cleaved cytokeratin 18 with the TUNEL method for quantification of apoptosis in histological sections of PC-3 subcutaneous xenografts. J. Pathol. 199, 221–228.

Eisen, J.S., Smith, J.C., 2008. Controlling morpholino experiments: do not stop making antisense. Development 135, 1735–1743.

Elsea, S.H., Girirajan, S., 2008. Smith–Magenis syndrome. Eur. J. Hum. Genet. 16, 412–421.

Elsea, S.H., Purandare, S.M., Adell, R.A., Juyal, R.C., Davis, J.G., Finucane, B., Magenis, R.E., Patel, P.I., 1997. Definition of the critical interval for Smith–Magenis syndrome. Cytogenet. Cell Genet. 79, 276–281.

Fieber, L.A., Tanguay, R.L., Walter, R.B., Williams, D.E., 2012. Aquatic animal models of human disease: selected papers from the 5th conference preface. Comp. Biochem. Physiol. C-Toxicol. Pharmacol. 155, 9–10.

Gato, A., Desmond, M.E., 2009. Why the embryo still matters: CSF and the neuroepithelium as interdependent regulators of embryonic brain growth, morphogenesis and histiogenesis. Dev. Biol. 327, 263–272.

Girirajan, S., Elsea, S.H., 2009. Abnormal maternal behavior, altered sociability, and impaired serotonin metabolism in Rai1-transgenic mice. Mamm. Genome 20, 247–255.

Girirajan, S., Vlangos, C.N., Szomju, B.B., Edelman, E., Trevors, C.D., Dupuis, L., Nezarati, M., Bunyan, D.J., Elsea, S.H., 2006. Genotype-phenotype correlation in Smith–Magenis syndrome: evidence that multiple genes in 17p11.2 contribute to the clinical spectrum. Genet. Med. 8, 417–427.

Glover, J.C., Renaud, J.S., Rijli, F.M., 2006. Retinoic acid and hindbrain patterning. J. Neurobiol. 66, 705–725.

Gutzman, J.H., Sive, H., 2009. Zebrafish brain ventricle injection. J. Vis. Exp..

Hellsten, U., Harland, R.M., Gilchrist, M.J., Hendrix, D., Jurka, J., Kapitonov, V., Ovcharenko, I., Putnam, N.H., Shu, S.Q., Taher, L., Blitz, I.L., Blumberg, B., Dichmann, D.S., Dubchak, I., Amaya, E., Detter, J.C., Fletcher, R., Gerhard, D.S., Goodstein, D., Graves, T., Grigoriev, I.V., Grimwood, J., Kawashima, T., Lindquist, E., Lucas, S.M., Mead, P.E., Mitros, T., Ogino, H., Ohta, Y., Poliakov, A.V., Pollet, N., Robert, J., Salamov, A., Sater, A.K., Schmutz, J., Terry, A., Vize, P.D., Warren, W.C., Wells, D., Wills, A., Wilson, R.K., Zimmerman, L.B., Zorn, A.M., Grainger, R., Grammer, T., Khokha, M.K., Richardson, P.M., Rokhsar, D.S., 2010. The genome of the Western clawed frog *Xenopus tropicalis*. Science 328, 633–636.

Hittner, H.M., King, R.A., Riccardi, V.M., Ledbetter, D.H., Borda, R.P., Ferrell, R.E., Kretzer, F.L., 1982. Oculocutaneous albinoidism as a manifestation of reduced neural crest derivatives in the Prader–Willi syndrome. Am. J. Ophthalmol. 94, 328–337.

Hu, C.J., Sataur, A., Wang, L., Chen, H., Simon, M.C., 2007. The N-terminal transactivation domain confers target gene specificity of hypoxia-inducible factors HIF-1alpha and HIF-2alpha. Mol. Biol. Cell 18, 4528–4542.

Huang, J.K., Dorey, K., Ishibashi, S., Amaya, E., 2007. BDNF promotes target innervation of *Xenopus mandibular* trigeminal axons in vivo. BMC Dev. Biol. 7, 59.

Ichim, G., Tauszig-Delamasure, S., Mehlen, P., 2012. Neurotrophins and cell death. Exp. Cell Res. 318, 1221–1228.

Imai, Y., Suzuki, Y., Matsui, T., Tohyama, M., Wanaka, A., Takagi, T., 1995. Cloning of a retinoic acid-induced gene, Gt1, in the embryonal carcinoma cell-line P19 – neuron-specific expression in the mouse–brain. Mol. Brain Res. 31, 1–9.

Jernigan, T.L., Bellugi, U., 1990. Anomalous brain morphology on magnetic-resonance images in Williams syndrome and down syndrome. Arch. Neurol. 47, 529–533.

Juyal, R.C., Figuera, L.E., Hauge, X., Elsea, S.H., Lupski, J.R., Greenberg, F., Baldini, A., Patel, P.I., 1996. Molecular analyses of 17p11.2 deletions in 62 Smith–Magenis syndrome patients. Am. J. Hum. Genet. 58, 998–1007.

Kaltenbrun, E., Tandon, P., Amin, N.M., Waldron, L., Showell, C., Conlon, F.L., 2011. *Xenopus*: an emerging model for studying congenital heart disease. Birth Defects Res. Part a-Clin. Mol. Teratol. 91, 495–510.

Kennedy, A.E., Dickinson, A.J., 2012. Median facial clefts in *Xenopus laevis*: roles of retinoic acid signaling and homeobox genes. Dev. Biol. 365, 229–240.

Kennedy, A.E., Dickinson, A.J., 2014. Quantitative analysis of orofacial development and median clefts in *Xenopus laevis*. Anat. Rec. (Hoboken) 297, 834–855.

Khokha, M.K., 2012. *Xenopus* white papers and resources: folding functional genomics and genetics into the frog. Genesis 50, 133–142.

Klingenberg, C.P., 2011. MorphoJ: an integrated software package for geometric morphometrics. Mol. Ecol. Resour. 11, 353–357.

Klingenberg, C.P., Wetherill, L., Rogers, J., Moore, E., Ward, R., Autti-Ramo, I., Fagerlund, A., Jacobson, S.W., Robinson, L.K., Hoyme, H.E., Mattson, S.N., Li, T.K., Riley, E.P., Foroud, T., 2010. Prenatal alcohol exposure alters the patterns of facial asymmetry. Alcohol 44, 649–657.

Kochilas, L., Merscher-Gomez, S., Lu, M.M., Potluri, V., Liao, J., Kucherlapati, R., Morrow, B., Epstein, J.A., 2002. The role of neural crest during cardiac development in a mouse model of DiGeorge syndrome. Dev. Biol. 251, 157–166.

Laje, G., Morse, R., Richter, W., Ball, J., Pao, M., Smith, A.C., 2010. Autism spectrum features in Smith–Magenis syndrome. Am. J. Med. Genet. C Semin. Med. Genet. 154C, 456–462.

Lim, J.H., Luo, T., Sargent, T.D., Fallon, J.R., 2005. Developmental expression of *Xenopus fragile* X mental retardation-1 gene. Int. J. Dev. Biol. 49, 981–984.

Lindsay, R.M., 1996. Role of neurotrophins and trk receptors in the development and maintenance of sensory neurons: an overview. Philos. Trans. R. Soc. Lond. B Biol. Sci. 351, 365–373.

Lowery, L.A., Sive, H., 2009. Totally tubular: the mystery behind function and origin of the brain ventricular system. BioEssays 31, 446–458.

Mark, M., Ghyselinck, N.B., Chambon, P., 2004. Retinoic acid signalling in the development of branchial arches. Curr. Opin. Genet. Dev. 14, 591–598.

Martinez-Morales, P.L., del Corral, R.D., Olivera-Martinez, I., Quiroga, A.C., Das, R.M., Barbas, J.A., Storey, K.G., Morales, A.V., 2011. FGF and retinoic acid activity gradients control the timing of neural crest cell emigration in the trunk. J. Cell Biol. 194, 489–503.

Musselman, C.A., Kutateladze, T.G., 2009. PHD fingers epigenetic effectors and potential drug targets. Mol. Interventions 9, 314–323.

Nieuwkoop, P.D., Faber, J., 1967. Normal table of *Xenopus laevis* (Daudin). Garland Publishing Inc., New York, p. 263.

Pratt, K.G., Khakhalin, A.S., 2013. Modeling human neurodevelopmental disorders in the Xenopus tadpole: from mechanisms to therapeutic targets. Dis. Models Mech. 6, 1057–1065.

Renato Ocampo, J. and Persing, J.A. 1997. Hypertelorism. In: Bentz, M.L. (Ed.), Pediatric Plastic Surgery, McGraw-Hill Professional, New York.

Roper, R.J., VanHorn, J.F., Cain, C.C., Reeves, R.H., 2009. A neural crest deficit in down syndrome mice is associated with deficient mitotic response to Sonic hedgehog. Mech. Dev. 126, 212–219.

Santoriello, C., Zon, L.I., 2012. Hooked! modeling human disease in zebrafish. J. Clin. Invest. 122, 2337–2343.

Seidl, R., Bidmon, B., Bajo, M., Yoo, B.C., Cairns, N., LaCasse, E.C., Lubec, G., 2001. Evidence for apoptosis in the fetal down syndrome brain. J. Child Neurol. 16, 438–442.

Showell, C., Conlon, F.L., 2007. Decoding development in *Xenopus tropicalis*. Genesis 45, 418–426.

Sive, H., 2011. 'Model' or 'tool'? New definitions for translational research. Dis. Models Mech. 4, 137–138.

Sive, H.L., Grainger, R., Harland, R., 2000. Early development of *Xenopus laevis*: a laboratory manual. Cold Spring Harbor Laboratory Press.

Slager, R.E., Newton, T.L., Vlangos, C.N., Finucane, B., Elsea, S.H., 2003. Mutations in RAI1 associated with Smith–Magenis syndrome. Nat. Genet. 33, 466–468.

Summerton, J.E., 2007. Morpholino, siRNA, and S-DNA compared: impact of structure and mechanism of action on off-target effects and sequence specificity. Curr. Top. Med. Chem. 7, 651–660.

Please cite this article in press as: Tahir, R. et al, Retinoic acid induced-1 (Rai1) regulates craniofacial and brain development in Xenopus, Mech. Dev. (2014), http://dx.doi.org/10.1016/j.mod.2014.05.004

Takeuchi, H., Mizuno, T., Zhang, G.Q., Wang, J.Y., Kawanokuchi, J., Kuno, R., Suzumura, A., 2005. Neuritic beading induced by activated microglia is an early feature of neuronal dysfunction toward neuronal death by inhibition of mitochondrial respiration and axonal transport. J. Biol. Chem. 280, 10444–10454.

Tandon, P., Showell, C., Christine, K., Conlon, F.L., 2012. Morpholino injection in *Xenopus*. Methods Mol. Biol. 843, 29–46.

Taylor, W., 1985. Revised procedures for staining and clearing small fishes and other vertebrates for bone and cartilage study. Cybium 9, 107–119.

Tropepe, V., Sive, H.L., 2003. Can zebrafish be used as a model to study the neurodevelopmental causes of autism? Genes Brain Behav 2, 268–281.

Wang, J.T., Medress, Z.A., Barres, B.A., 2012. Axon degeneration: molecular mechanisms of a self-destruction pathway. J. Cell Biol. 196, 7–18.

Wilkins, B.J., Pack, M., 2013. Zebrafish models of human liver development and disease. Compr. Physiol. 3, 1213–1230.

Winning, R.S., Shea, L.J., Marcus, S.J., Sargent, T.D., 1991. Developmental regulation of transcription factor AP-2 during *Xenopus laevis* embryogenesis. Nucleic Acids Res. 19, 3709–3714.

Wurdak, H., Ittner, L.M., Lang, K.S., Leveen, P., Suter, U., Fischer, J.A., Karlsson, S., Born, W., Sommer, L., 2005. Inactivation of TGFbeta signaling in neural crest stem cells leads to multiple defects reminiscent of DiGeorge syndrome. Genes Dev. 19, 530–535.

Yamada, K., Matsuzawa, H., Uchiyama, M., Kwee, I.L., Nakada, T., 2006. Brain developmental abnormalities in Prader–Willi syndrome detected by diffusion tensor imaging. Pediatrics 118, E442–E448.

Yan, J., Bi, W., Lupski, J.R., 2007. Penetrance of craniofacial anomalies in mouse models of Smith–Magenis syndrome is modified by genomic sequence surrounding Rai1: not all null alleles are alike. Am. J. Hum. Genet. 80, 518–525.

Zon, L.I., 1999. Zebrafish: a new model for human disease. Genome Res. 9, 99–100.

Please cite this article in press as: Tahir, R. et al, Retinoic acid induced-1 (Rai1) regulates craniofacial and brain development in Xenopus, Mech. Dev. (2014), http://dx.doi.org/10.1016/j.mod.2014.05.004